Proceedings of the Institution of Civil Engineers
Structures and Buildings 163
August 2010 Issue SB4
Pages 245–255
doi: 10.1680/stbu.2010.163.4.245

Paper 900049
Received 21/05/2009
Accepted 07/09/2009

Keywords: composite structures/ design methods & aids/timber structures

Digby Symons
University of Cambridge, Department of Engineering, Cambridge, UK

Richard Persaud
Ramboll UK, Cambridge, UK

Harsha Stanislaus
University of Cambridge, Department of Engineering, Cambridge, UK

ice
Institution of Civil Engineers

Slip modulus of inclined screws in timber–concrete floors

D. Symons MA, DPhil, CEng, MIMechE, R. Persaud MPhil, PhD and H. Stanislaus MEng

This paper presents a model for the stiffness of inclined screws used as shear connectors in timber and concrete composite floors. Screws inclined in the direction of slip have been shown to provide a higher stiffness (slip modulus) than vertically placed screws. An increased slip modulus per screw enhances the effective flexural stiffness of a partially composite timber and concrete beam, or, alternatively, allows the same flexural stiffness to be achieved with fewer screws. The model assumes that the screw behaves as a beam on a two-dimensional elastic foundation: it takes account of the inclination of the screw and models the timber as orthogonal springs with differing stiffnesses in the grain and transverse directions. The model also considers axial deformation, and hence shear lag, of the screw. Optimum inclination angle and embedment length of screw can be predicted. Preliminary validation of the model is provided by comparison with some experimental results.

NOTATION

A	cross-sectional area of screw ($A = \pi d^2/4$)
d	diameter of screw shank
E	Young's modulus of screw material ($\hat{E} = E/k_p$)
E_p	elastic modulus of timber parallel to the grain
$(EI)_{ef}$	effective flexural stiffness of a partially composite beam
I	second moment of area of screw cross-section ($I = \pi d^4/64$)
K	slip modulus ($K = R/u$)
k_p	foundation modulus of timber parallel to the grain (stiffness per unit length)
k_t	foundation modulus of timber transverse to the grain (stiffness per unit length)
M	bending moment in screw
R	shear force between timber and concrete
S	shear force in screw
T	axial force in screw
t	length of screw embedded in timber ($\hat{t} = t/d$)
u	slip at interface between timber and concrete
v	axial displacement of screw
w	lateral displacement of screw
x	distance along screw from the timber/concrete interface
β	ratio of foundation moduli ($\beta = k_t/k_p$)
γ	characteristic length for axial deformation ($\hat{\gamma} = \gamma/d$)
λ	characteristic length for transverse deformation ($\hat{\lambda} = \lambda/d$)
θ	angle of inclination of screw from the vertical
ρ_m	density of timber

1. INTRODUCTION

This paper describes a theoretical model for calculating the stiffness (slip modulus) of inclined screws when used as shear connectors in timber–concrete composite floors or beams. The model considers the initial response of the connection, before any inelastic behaviour.

1.1. Timber–concrete composites

Timber–concrete composite construction consists of timber members in the tensile zone, a concrete slab in the compression zone and a shear connection between the timber and the concrete. Timber–concrete composite floors can be attractive for both refurbishment and new-build projects. In refurbishment projects the installation of shear connectors followed by the in situ casting of a concrete slab upon existing timber joists can offer a cost-effective route to increase the stiffness, strength and fire resistance of an existing timber floor. In new-build applications a timber–concrete composite floor system can offer a reduction in embodied carbon when compared with steel or concrete construction and superior noise insulation and thermal mass when compared with an all-timber solution.

Design of timber–concrete composite sections generally requires consideration of partial composite action; this is attributable to the difficulty of achieving an extremely rigid shear connection between the concrete and timber. Eurocode 5 (British Standards Institution (BSI), 2004) adopts the approximate 'gamma method' where an effective flexural stiffness $(EI)_{ef}$ for the composite section is calculated as a function of the stiffness (slip modulus) of the shear connection. The higher the stiffness of the shear connection the closer the effective flexural stiffness will be to that of a fully composite section.

1.2. Shear connection stiffness

A number of alternative shear connection systems have been proposed for timber–concrete composites; Persaud (2006) gives a broad review. These include combinations of discrete nails, screws, purpose-designed connectors, grooves cut into the timber and post-tensioned, glued-in dowels, as well as types of continuous mechanical connection. An example of the latter is TiComTec's 'HBV system', as tested by Bathon and Clouston (2004) and Clouston *et al.* (2004). This is a continuous

connection which consists of a strip of steel mesh glued into a slot cut into the top surface of the timber. This type of system has been shown to have excellent stiffness, strength and ductility, but is probably most appropriate for use in a pre-cast timber–concrete composite section.

Probably the simplest form of shear connection system that can be adopted is a line of screws placed at intervals along the beam, either self-tapping or into pre-drilled holes. Screws have the advantage of being readily available and easily installed. Although a continuous system can potentially offer superior stiffness and strength, a line of discrete screws will generally be more practical for installation into existing timber floor planks and joists in a refurbishment project. Discrete screws can also be used conveniently in combination with profiled steel decking as permanent formwork for a new-build application, as tested by Persaud and Symons (2006).

Screw shear connectors would conventionally be installed vertically. A drawback of vertical placement is that the relative slip between timber and concrete is primarily resisted by bending of the screw and this leads to low slip stiffness. However, if the screws are inclined in the direction of shear loading (as shown in Figure 1) then the screws are loaded axially as well as in bending. Tests reported by Meierhofer (1993), Fontana and Frangi (2003) and Steinberg *et al.* (2003) show that inclined screws can have significantly higher shear stiffness than vertical ones.

There is limited information in the literature and design codes on the stiffness of shear connectors, and in particular for inclined screws. Eurocode 5 does offer an empirical equation (Equation 1) for the slip modulus of dowels, screws or nails

$$K = \frac{2}{23}\rho_{\mathrm{m}}^{1{\cdot}5} d \qquad (1)$$

However, this equation is only for vertically driven connections, and takes no account of the length of the screw. In a commentary on the design of timber–concrete composite beams Ceccotti *et al.* (2002) simply recommend that experimental measurements of slip modulus be obtained. There therefore appears to be scope for development of a theoretical approach that can explain the dependency of the slip modulus of a screw on both its length and angle of inclination and hence offer insight for designers.

This paper proposes a theoretical approach that is based on the well-known 'Winkler' foundation, or beam on an elastic foundation. A number of previous authors have proposed using a Winkler foundation to model the deformation of a vertically placed screw (or dowel) embedded in timber under lateral load; these include Kuenzi (1951), Patton-Mallory *et al.* (1997) and, more recently, Gelfi *et al.* (2002). The beam models the screw, which deforms primarily in bending, while the elastic foundation of independent springs represents the resistance of the grain of the timber to lateral (horizontal) movement of the screw (Figure 2). To extend this model to the problem of an inclined screw requires an additional set of springs which resist movement of the screw in the vertical direction, that is transverse to the grain (Figure 3). It is noted in passing that a precedent for using a Winkler foundation to represent the stiffness of timber transverse to the grain may be found in models of transverse timber splitting; authors include Blass and Schmid (2001), Jensen and Gustafsson (2004) and Jensen 2005).

1.3. Foundation modulus

The stiffness of the foundation springs in a Winkler foundation model may be termed the subgrade or foundation modulus.

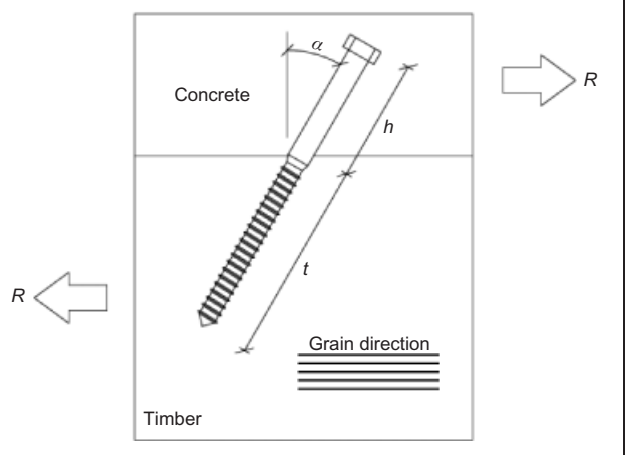

Figure 1. Coach screw inserted into timber in the direction of slip

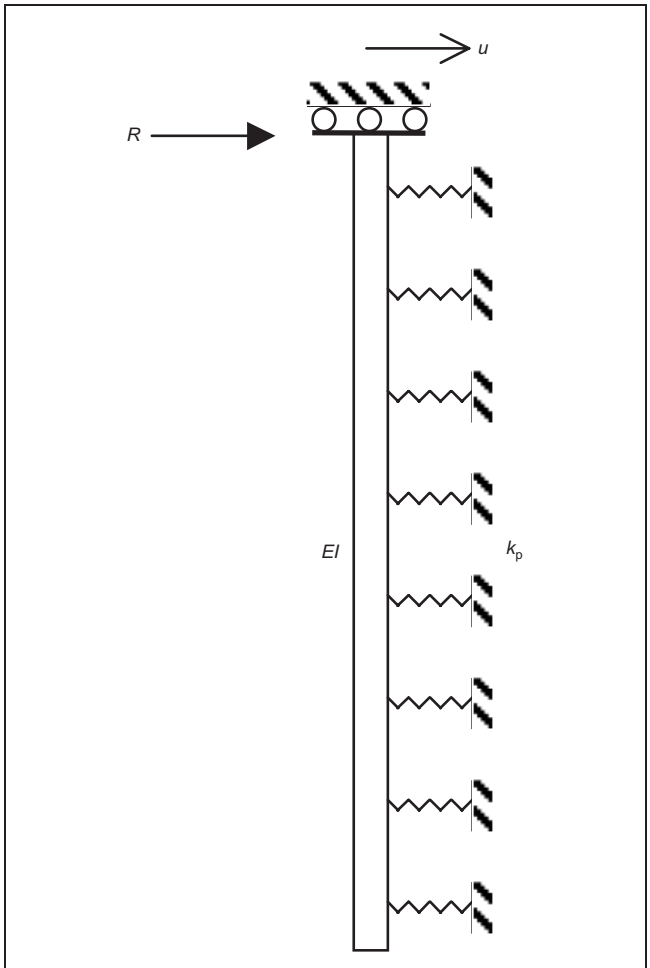

Figure 2. Vertical screw modelled as a beam on elastic foundation

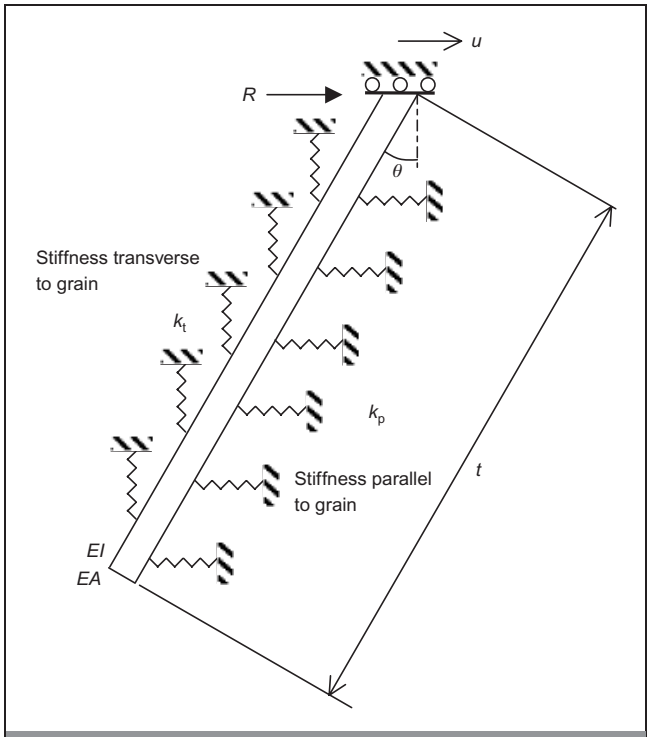

Figure 3. Model of inclined screw on elastic foundations

Measurements of the initial resistance of timber to lateral displacement of a screw or dowel can be used to obtain the foundation modulus. Table 1 details measured moduli, parallel (k_p) and transverse (k_t) to the grain, reported in four different studies. In each case a short steel dowel was translated laterally through a thin plank of softwood and the initial force/displacement response recorded. The foundation modulus is obtained by dividing the measured stiffness by the thickness of the timber plank. The measurements of modulus parallel to the grain (k_p) are broadly consistent between the four studies. It is particularly interesting to note the results of Gelfi *et al.* (2002) who found that the modulus does not significantly depend on the diameter of dowel (they tested dowels of 12, 16, 20 and 48 mm diameter). The ratio $\beta = k_t/k_p$ of the orthogonal moduli ranges from 0·33 for pine (Santos *et al.*, 2010) to around 0·6 for spruce (Gattesco, 1998; Gattesco and Toffolo, 2004); on this basis a value of $\beta = 0{\cdot}5$ seems an appropriate general value for softwood.

1.4. Outline of the current paper

An outline of this paper is as follows. First the inclined beam on an elastic foundation model is described. Two limiting cases are considered in turn: a relatively short screw where axial deformation of the screw can be neglected, and a very long screw where axial deformation is significant and bending of the screw may be neglected. These cases are then combined into a general model for screws of any length. The predictions of the model are then compared with some experimental results.

2. DESCRIPTION OF MODEL

2.1. Problem definition

Figure 3 represents the model of a screw inclined at an angle θ to the vertical. The timber grain direction is horizontal. It is assumed that the upper portion of the screw embedded in concrete is rigidly held, and therefore that it is only necessary to model the length t of the screw that is embedded in timber (concrete is typically around four times stiffer than structural timber and the substantial head of a typical coach screw is expected to provide significant restraint). A shear force R is applied at the interface between timber and concrete, which results in a horizontal slip displacement u. The screw has flexural rigidity EI and axial stiffness EA. If the diameter of the screw shank is d then $A = \pi d^2/4$ and $I = \pi d^4/64$.

Figure 4 shows an element of the part of the inclined screw that is embedded within the timber. The element is of length δx and a distance x from the interface of the timber and concrete. w and v are the transverse and axial displacements of the element within the timber. These displacements are assumed to be resisted by a set of independent spring stiffnesses in the horizontal (parallel to the grain) and vertical (transverse to the grain) directions. The stiffnesses of these springs, per unit length, are k_p and k_t, respectively. Axial force, shear force and bending moment stress resultants are represented by the variables T, S and M, respectively.

The horizontal and vertical restoring forces on the element are $(w\cos\theta + v\sin\theta)k_p\delta x\cos\theta$ and $(v\cos\theta - w\sin\theta)k_t\delta x\sin\theta$, respectively. The rate of change of shear force S along the length of screw is therefore given by Equation 2

Study	Gattesco (1998)	Gattesco and Toffolo (2004)	Gelfi *et al.* (2002)	Santos *et al.* (2010)
Timber species	Eastern Alps spruce	Glulam eastern Alps red spruce	Alps spruce	Pine (*Pinus pinaster*)
Density of timber	469 kg/m^3	442 kg/m^3	–	560 kg/m^3
Moisture content	12·1%	9·9%	–	12%
Young's modulus parallel to the grain E_p	13·1 GPa	13·9 GPa	–	15·1 GPa
Diameter of testing dowel	16 mm	16 mm	12 to 48 mm	14 mm
Foundation modulus parallel to the grain k_p	1210 N/mm^2	1320 N/mm^2	1300 N/mm^2	1590 N/mm^2
Foundation modulus transverse to the grain k_t	763 N/mm^2	732 N/mm^2	–	521 N/mm^2
Ratio of moduli $\beta = \frac{k_t}{k_p}$	0·63	0·56	–	0·33

Table 1. Reported measurements of timber foundation stiffness

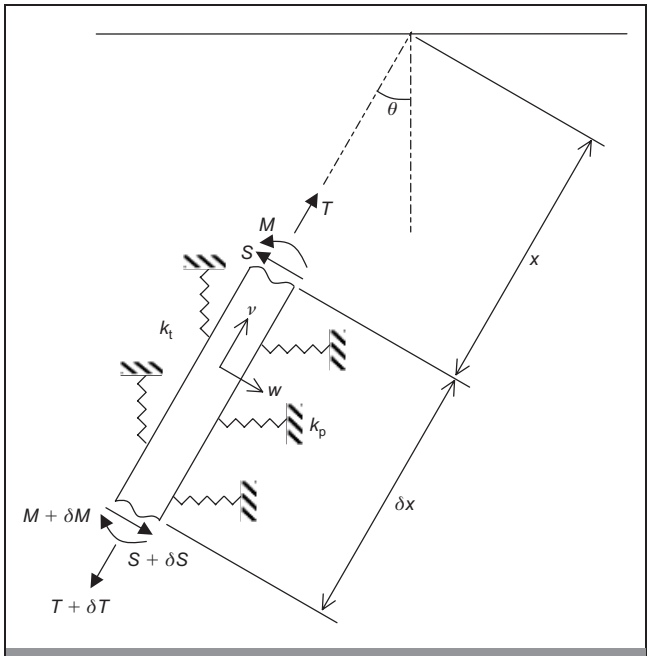

Figure 4. Element of inclined screw within timber

$$\frac{dS}{dx} = -EI\frac{d^4w}{dx^4} = (w\cos\theta + v\sin\theta)k_p\cos^2\theta - (v\cos\theta - w\sin\theta)k_t\sin^2\theta \quad (2)$$

This may be expressed as a differential equation (Equation 3) for transverse deflection w

$$\frac{d^4w}{dx^4} + \frac{4}{\lambda^4}w = \frac{\cos\theta\sin\theta}{EI} \times (k_t\sin\theta - k_p\cos\theta)v \quad (3)$$

where the characteristic length λ is given by Equation 4

$$\lambda = \sqrt[4]{\frac{4EI}{k_p\cos^3\theta + k_t\sin^3\theta}} \quad (4)$$

The rate of change of axial force along the screw is given by Equation 5

$$\frac{dT}{dx} = -\left[(w\cos\theta + v\sin\theta)k_p + (v\cos\theta - w\sin\theta)k_t\right]\sin\theta\cos\theta \quad (5)$$

At the interface of the timber and concrete $x = 0$ and the axial and shear force in the screw are T_0 and S_0, respectively. Neglecting friction between the timber and concrete the horizontal shear force R is given by Equation 6

$$R = T_0\sin\theta - S_0\cos\theta \quad (6)$$

It is assumed that the slip at the interface is constrained to be a purely horizontal displacement u, so that $w = w_0 = u\cos\theta$ and $v = v_0 = u\sin\theta$ at $x = 0$.

Note that only the horizontal forces corresponding to a single connector are resolved and the full equilibrium of either the timber or concrete sections is not considered. Eccentricity of the external shear force applied to these sections would introduce corresponding (although small) normal forces at the interface spread over multiple connectors and these are not relevant to this model.

2.2. Transverse deflection model

In the case of a screw which is not very long (e.g. $t/d < 20$) it can be assumed that the screw is inextensional; thus the axial displacement v is constant over the length of the screw so that $v = v_0 = u\sin\theta$ for all x. Additional boundary conditions are as follows:

$$\text{at } x = 0\text{: } \frac{dw}{dx} = 0,\ S_0 = -EI\frac{d^3w}{dx^3};\quad \text{and at } x = t\text{: } \frac{d^3w}{dx^3} = \frac{d^2w}{dx^2} = 0 \quad (7)$$

A solution (Equation 7) to Equation 3 that matches these boundary conditions may be found with reference to Hetenyi (1946).

$$w = \frac{1}{(k_p\cos^3\theta + k_t\sin^3\theta)} \times \left\{ \begin{array}{l} \dfrac{-S_0}{\lambda(\sinh(2t/\lambda) + \sin(2t/\lambda))} \times \\ \left[\begin{array}{c} \cosh(x/\lambda)\cos\big((2t-x)/\lambda\big) \\ +\cos(x/\lambda)\cosh\big((2t-x)/\lambda\big) \\ -\sinh(x/\lambda)\sin\big((2t-x)/\lambda\big) \\ +\sin(x/\lambda)\sinh\big((2t-x)/\lambda\big) \\ +2\cosh(x/\lambda)\cos(x/\lambda) \end{array} \right] \\ +u\cos\theta\sin^2\theta[k_p\sin\theta - k_t\cos\theta] \end{array} \right\} \quad (7)$$

Since $w_0 = u\cos\theta$ the interface shear force may be obtained (Equation 8)

$$S_0 = -\lambda k_p u\cos^2\theta \times \frac{(\sinh 2t/\lambda + \sin 2t/\lambda)}{(\cosh 2t/\lambda + \cos 2t/\lambda + 2)} \quad (8)$$

The interface axial force T_0 (Equation 9) can be found by substituting Equation 7 into Equation 5 and integrating, subject to the boundary condition that $T = 0$ at $x = t$

$$T_0 = \left[\frac{utk_pk_t\sin\theta - S_0(k_p\cos\theta - k_t\sin\theta)}{k_p\cos^3\theta + k_t\sin^3\theta}\right] \times \sin\theta\cos\theta \quad (9)$$

Substitution of Equations 8 and 9 into Equation 6 gives an expression (Equation 10) for the slip modulus K_{inex} of an inextensional screw. This expression considers only the bending deformation of the screw.

10
$$K_{\text{inex}} = \frac{R}{u} = \frac{k_p \cos\theta}{1+\beta\tan^3\theta} \times \left[\lambda \frac{(\sinh 2t/\lambda + \sin 2t/\lambda)}{(\cosh 2t/\lambda + \cos 2t/\lambda + 2)} + t\beta\tan^3\theta\right]$$

where

11
$$\beta = \frac{k_t}{k_p}$$

2.3. Axial shear lag model for very long screws

In the case of a very long (e.g. $t/d > 40$) inclined screw axial deformation of the screw will become important and provide a limit on the gains in stiffness, which can be made by continuing to increase the length t.

Over most of the length of a very long screw the shear force $S \approx 0$. Hence from Equation 2 a fixed relationship is obtained (Equation 12) between the lateral and axial displacements w and v.

12
$$w(1+\beta\tan^3\theta) = -v(1-\beta\tan\theta)\tan\theta$$

By substitution of Equation 12 into Equation 5, and noting that $T = -EA\frac{dv}{dx}$, a differential equation for the axial deformation v can be obtained (Equation 13)

13
$$\frac{d^2v}{dx^2} - \frac{v}{\gamma^2} = 0$$

where γ is a characteristic length

14
$$\gamma = \sqrt{\frac{(1+\beta\tan^3\theta)}{\beta\tan\theta}\frac{EA}{k_p}\cos\theta}$$

Noting the boundary condition that $T = 0$ at $x = t$ gives a solution (Equation 15) for the axial force T_0 at the root

15
$$T_0 = \frac{v_0}{\gamma} EA \tanh\frac{t}{\gamma}$$

By recalling the assumption that $S \approx 0$ throughout and that $v_0 = u\sin\theta$ an expression (Equation 16) is therefore obtained for the slip modulus K_{long} of a very long screw. This expression considers only axial deformation of the screw and neglects bending deformation of the screw

16
$$K_{\text{long}} = \frac{R}{u} = \frac{EA}{\gamma}\tanh\left(\frac{t}{\gamma}\right)\sin^2\theta$$

For $t > \gamma$ $\tanh(t/\gamma) \to 1$ very quickly and therefore there is a definite upper limit on the slip modulus due to axial withdrawal of $EA\sin^2\theta/\gamma$.

2.4. Combined model

It is also noted that as

17
$$\frac{t}{\gamma} \to \quad \frac{EA}{\gamma}\tanh\left(\frac{t}{\gamma}\right)\sin^2\theta \to k_p t\cos\theta\frac{\beta\tan^3\theta}{1+\beta\tan^3\theta}$$

and therefore for small values of t/γ Equation 16 is approximately equal to the second term of Equation 10. This leads us to a single, combined model (Equation 18) for the slip modulus K, which should be valid for any length of inclined screw.

18
$$K = \frac{R}{u} = \frac{k_p\cos\theta}{1+\beta\tan^3\theta} \times \lambda\frac{(\sinh 2t/\lambda + \sin 2t/\lambda)}{(\cosh 2t/\lambda + \cos 2t/\lambda + 2)} + \frac{EA}{\gamma}\tanh\left(\frac{t}{\gamma}\right)\sin^2\theta$$

For generality it is convenient to express Equation 18 as a non-dimensional slip modulus $\hat{K} = K/k_p d$

19
$$\hat{K} = \frac{K}{k_p d} = \frac{\cos\theta}{(1+\beta\tan^3\theta)} \times \hat{\lambda}\frac{\left(\sinh 2\hat{t}/\hat{\lambda} + \sin 2\hat{t}/\hat{\lambda}\right)}{\left(\cosh 2\hat{t}/\hat{\lambda} + \cos 2\hat{t}/\hat{\lambda} + 2\right)} + \frac{\pi\hat{E}}{4\hat{\gamma}}\tanh\left(\frac{\hat{t}}{\hat{\gamma}}\right)\sin^2\theta$$

where $\hat{t} = t/d$ is the non-dimensional screw length, $\hat{\lambda} = \lambda/d$ (Equation 20) and $\hat{\gamma} = \gamma/d$ (Equation 21) are the non-dimensional characteristic lengths (which nevertheless remain functions of θ) and $\hat{E} = E/k_p$ is the ratio of the Young's modulus to the foundation modulus of the timber.

20
$$\hat{\lambda} = \frac{\lambda}{d} = \frac{1}{2}\sqrt[4]{\hat{E}\frac{\pi}{\cos^3\theta(1+\beta\tan^3\theta)}}$$

21
$$\hat{\gamma} = \frac{\gamma}{d} = \frac{1}{2}\sqrt{\hat{E}\frac{\pi(1+\beta\tan^3\theta)\cos\theta}{\beta\tan\theta}}$$

2.5. Interpretation of the model

The ratios $\hat{E}$ and β are key parameters that are fixed by the choice of screw and timber material. For steel screws in softwood values of $\hat{E} = 150$ and $\beta = 0{\cdot}5$ would seem to be typical ($E = 200$ GPa, $k_p \sim 1300$ N/mm^2 , $k_t \sim 650$ N/mm^2). These are now fixed and an investigation is made into how the slip modulus $\hat{K}$ depends upon the length $\hat{t}$ and/or inclination θ of the screw.

It is instructive first to consider two limiting cases: a vertically driven screw ($\theta = 0$), and a very long screw ($\hat{t} \to \infty$). In the first case Equations 19 and 20 reduce to

for $\theta = 0$

$$\hat{K} = \hat{\lambda}\frac{\left(\sinh 2\hat{t}/\hat{\lambda} + \sin 2\hat{t}/\hat{\lambda}\right)}{\left(\cosh 2\hat{t}/\hat{\lambda} + \cos 2\hat{t}/\hat{\lambda} + 2\right)} \quad \text{and } \hat{\lambda} = \frac{1}{2}\sqrt[4]{\pi\hat{E}} \tag{22}$$

Figure 5 shows how the slip modulus $\hat{K}$ depends on embedment depth $\hat{t}$ for a vertical screw. Inset figures show the deformed shape of the screw for selected values of $\hat{t}$. For $\hat{t} < \hat{\lambda} = 2{\cdot}3$, there is negligible bending of the screw and $\hat{K} \approx \hat{t}$; however, if $\hat{t} > 4\hat{\lambda} = 9$ the deeply embedded portion of the screw becomes effectively fixed and the bending of the portion close to the interface gives $\hat{K} \approx \hat{\lambda}$. There is no benefit in increasing the embedment t beyond $9d$.

In the second case ($\hat{t} \to \infty$), Equation 19 can be re-written as for $\hat{t} = \infty$

$$\hat{K} = \frac{\cos\theta}{(1+\beta\tan^3\theta)}\hat{\lambda} + \frac{\pi}{4}\frac{\hat{E}}{\hat{\gamma}}\sin^2\theta = \frac{1}{2}\left\{\sqrt[4]{\frac{\pi\hat{E}\cos\theta}{(1+\beta\tan^3\theta)^5}} + \frac{1}{\cos\theta}\sqrt{\frac{\pi\beta\hat{E}\sin^5\theta}{1+\beta\tan^3\theta}}\right\} \tag{23}$$

This expression is plotted in Figure 6. The maximum value of slip modulus is $\hat{K} = 6{\cdot}1$ at an inclination of $\theta = 62°$; the optimally inclined screw is 2·6 times stiffer than the same screw when placed vertically.

Figure 7 shows a three-dimensional plot of $\hat{K}$ for a wide range of $\hat{t}$ and θ.

2.6. Effect of interface friction

Friction acting at the interface between timber and concrete will have the effect of increasing the resistance to initial slip and therefore increasing the apparent slip modulus. This effect may be included in the model if required. The normal force N acting between the components is given by

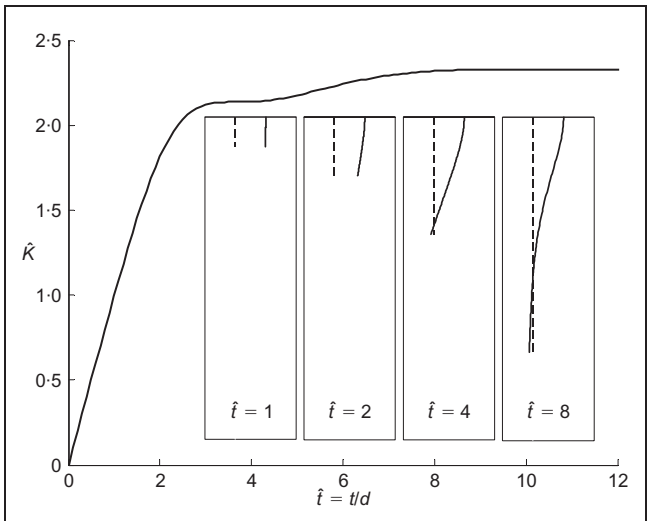

Figure 5. Non-dimensional stiffness $\hat{K}$ of a vertical screw ($\theta = 0$, $\hat{E} = 150$ and $\beta = 0{\cdot}5$)

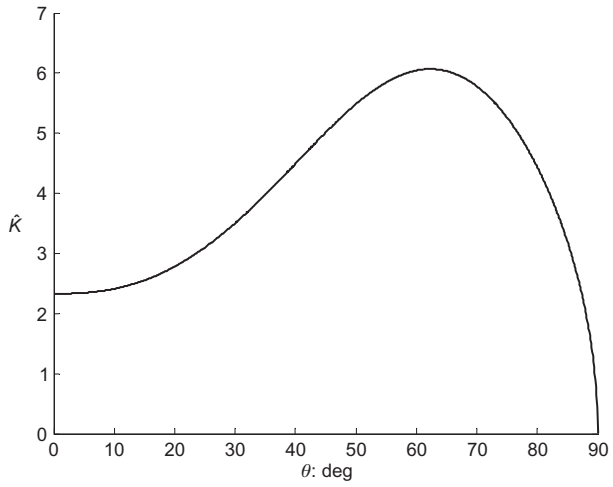

Figure 6. Non-dimensional stiffness $\hat{K}$ of a very long inclined screw ($\hat{t} \to \infty$, $\hat{E} = 150$ and $\beta = 0{\cdot}5$)

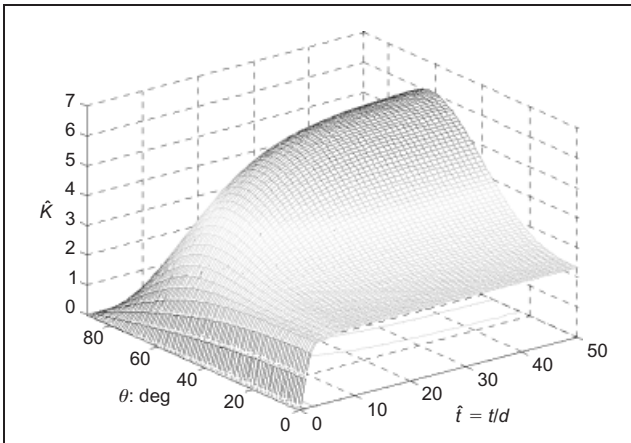

Figure 7. Non-dimensional stiffness $\hat{K}$ of an inclined screw ($\hat{E} = 150$ and $\beta = 0{\cdot}5$)

$$N = T_0\cos\theta + S_0\sin\theta \tag{24}$$

Equation 6 may then be modified to include the frictional force μN

$$R = T_0\sin\theta - S_0\cos\theta + \mu N = T_0(\sin\theta + \mu\cos\theta) - S_0(\cos\theta - \mu\sin\theta) \tag{25}$$

where μ is the coefficient of friction. This leads to an expression for the apparent slip modulus $\hat{K}_{\text{fric}} = K_{\text{fric}}/k_{\text{p}}d$ which includes the effect of friction

$$\frac{K_{\text{fric}}}{k_{\text{p}}d} = \frac{\cos\theta}{(1+\beta\tan^3\theta)} \times \hat{\lambda}\frac{\left(\sinh 2\hat{t}/\hat{\lambda} + \sin 2\hat{t}/\hat{\lambda}\right)}{\left(\cosh 2\hat{t}/\hat{\lambda} + \cos 2\hat{t}/\hat{\lambda} + 2\right)} \times \left(1 - \mu\beta\tan^2\theta\right) + \times\frac{\pi}{4}\frac{\hat{E}}{\hat{\gamma}}\tanh\left(\frac{\hat{t}}{\hat{\gamma}}\right)\sin^2\theta(1+\mu\cot\theta) \tag{26}$$

The magnitude of the influence of friction on the slip modulus is a function of the coefficient of friction μ. The apparent slip modulus $\hat{K}_{\text{fric}}$ is increased by up to 44% if $\mu = 1$, by 21% if $\mu = 0{\cdot}5$ and only 8% if $\mu = 0{\cdot}2$, relative to the frictionless modulus $\hat{K}$. Any contribution of friction is neglected when comparing the model with experimental results.

3. EXPERIMENTAL MEASUREMENTS

Two sets of experimental shear tests of inclined screws have been conducted to provide preliminary validation of the model. The first set used large 16 mm diameter, 230 mm long coach screws connecting structural glue-laminated timber to a concrete slab. These tests were intended to be representative of a practical application of inclined screw shear connectors in a timber and concrete composite floor. The second set of tests used smaller 6 mm diameter, 5 mm long coach screws in balsa wood.

3.1. Large-scale tests: 16 × 230 mm coach screws in glulam timber

3.1.1. Experimental method. The load–slip response of timber to concrete shear connections using inclined coach screws was investigated through a series of single-sided push-out shear tests. The test configuration is shown in Figure 8. The purpose of the experiments was to quantify the load–slip relationship of the shear connectors, and in particular to determine the shear stiffness (slip modulus), as well as the yield strength and ultimate strength.

The specimens tested were of a composite timber and concrete floor system utilising steel decking as permanent formwork for the concrete floor slab. Such a system was previously tested by the current authors with vertically inserted coach screws (Persaud and Symons, 2006). To construct each specimen a 1000 mm long, 600 mm wide and 100 mm deep concrete slab was cast on Richard Lees Holorib S280 0·9 mm permanent formwork steel decking. Each steel decking sheet was initially fixed to the timber beam with 4·5 mm × 20 mm long self-drilling, self-tapping screws, two per trough. In each trough of the decking, an ordinary 16 mm thread diameter, 230 mm long, coach screw was screwed into a pilot hole (pre-drilled in the timber to a depth $t \sim 120$ mm) to serve as a shear connector between the timber and concrete. The screw shank diameter $d = 12$ mm. There were a total of five coach screws in each specimen. To minimise eccentric loading (and consequent bending moment and axial loading of the screws) the load was applied as close as practically possible to the timber–concrete interface. Specimens were prepared with the coach screws inserted at angles of 0°, 10°, 20°, 30°, 40° and 50° to the vertical (see Figure 9, the use of Holorib decking limited the maximum inclination to 50°). Two identical specimens were made and tested for each angle. The glue-laminated timber beam was grade GL28, 270 × 160 mm in section and 1000 mm long. The average timber moisture content was 9·5%. The grain direction of the timber was parallel to the interface between concrete and timber. Further details of the experimental method are given in Symons *et al.* (2010) and Persaud (2006).

3.1.2. Results of experiments. The two specimens tested at each angle of inclination gave very similar responses. Figure 10 shows the load per connector against slip response of specimens with screws at 0°, 20° and 40° (plots for the other angles tested are omitted for clarity). The load was actually applied in repeated loading and unloading cycles of increasing amplitude; however, these cycles are removed from Figure 10 for clarity. Figure 11 shows details of the initial loading and unloading cycles for specimens with screws at 0° and 40°. Table 2 details experimental values for slip modulus for each specimen; these were obtained by measuring the gradient of a linear portion of a reloading cycle in the approximate range of 10 to 20 kN per screw.

3.1.3. Comparison of model with experimental results. The GL28 timber used in the test specimens had a measured (Persaud and Symons, 2006) elastic modulus parallel to the grain $E_{\text{p}} = 12{\cdot}1$ GPa. It is expected that the foundation modulus k_{p} will scale in proportion to E_{p} and therefore, by linear regression of the values in Table 1, the estimation $k_{\text{p}} \sim 1100$ N/mm^2 is made for this material and hence $\hat{E} = 180$ (steel screws

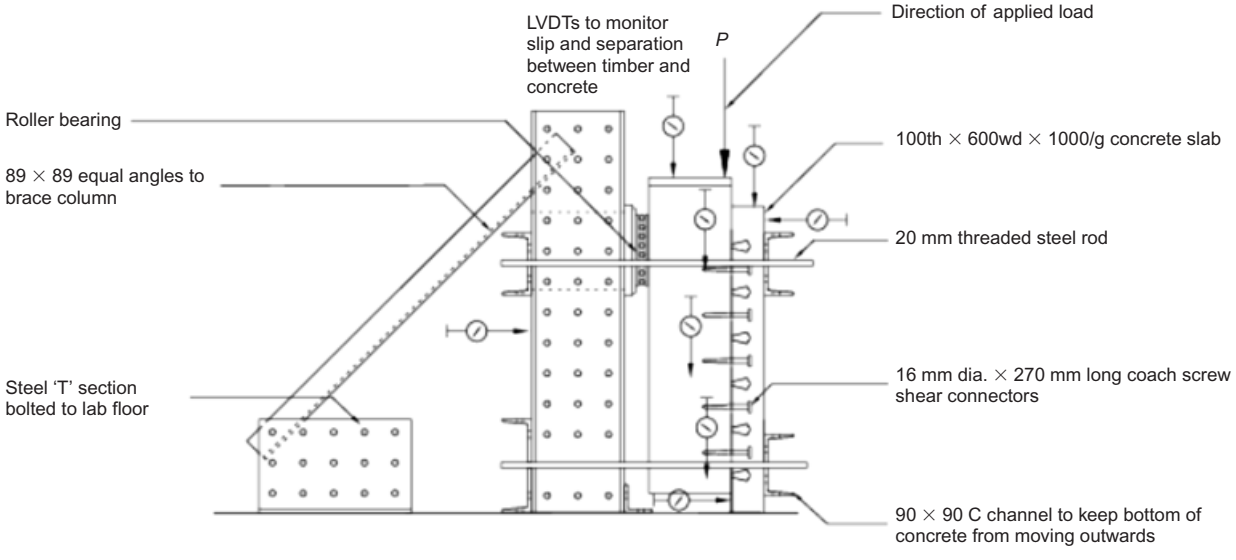

Figure 8. Single sided push-out test rig for large-scale tests

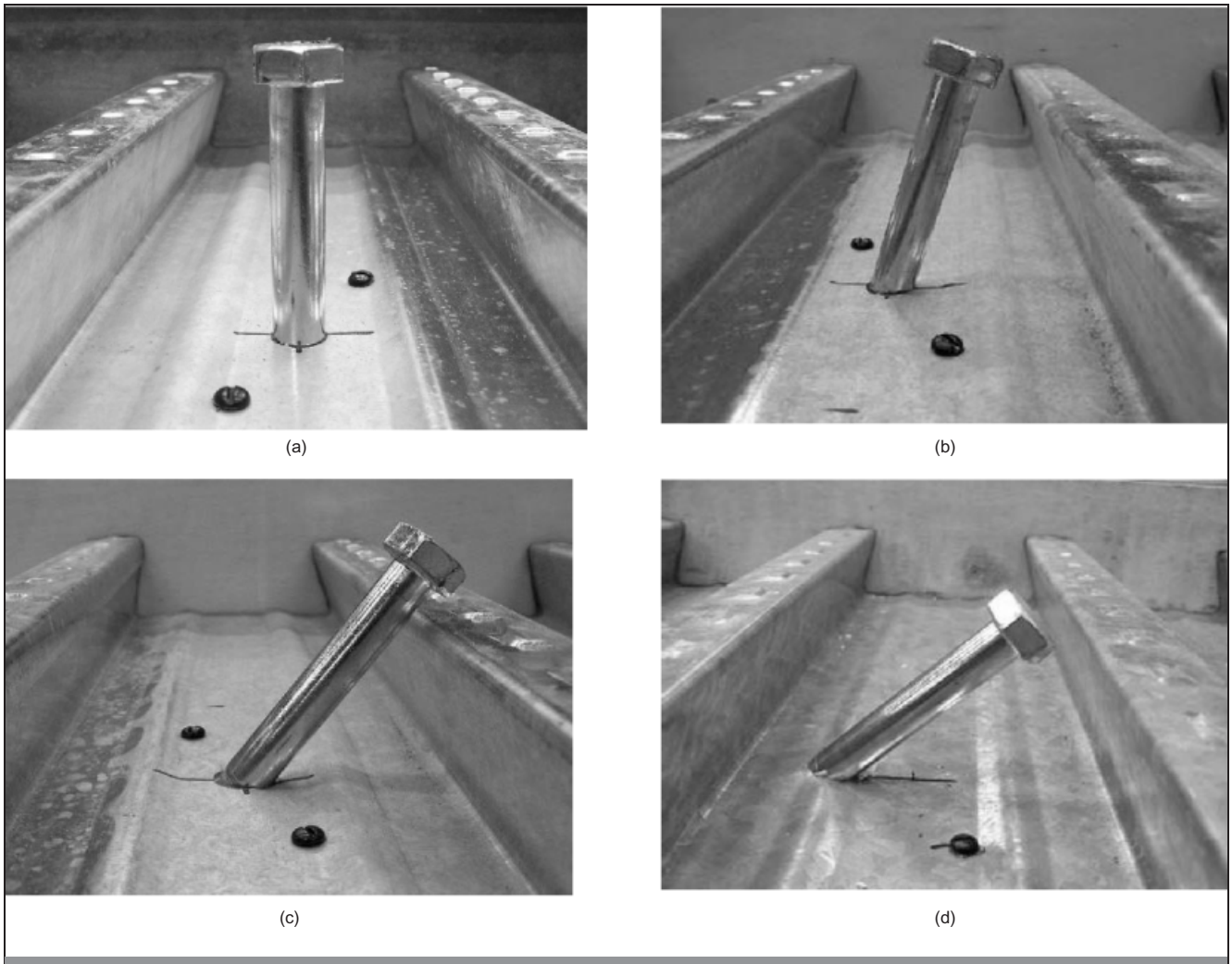

Figure 9 16 mm shear connector, Holorib decking and 4·5 mm temporary fixings: (a) vertical 16 mm screw; (b) 16 mm screw at 20° to the vertical; (c) 16 mm screw at 40° to the vertical; (d) 16 mm screw at 50° to the vertical

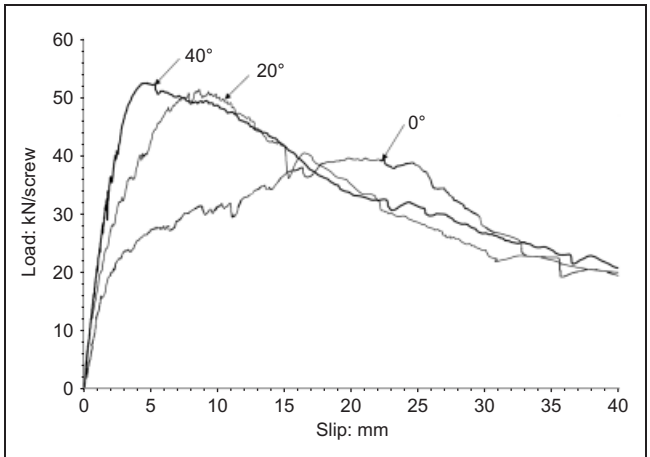

Figure 10. Load/slip response for 16 × 230 mm coach screws (no reloading cycles shown)

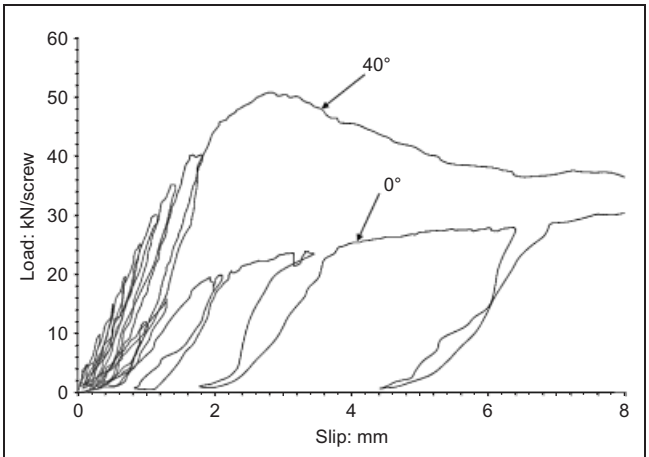

Figure 11. Load/slip response for 16 × 230 mm coach screws (with unload/reload cycles)

with $E = 200$ GPa). It is assumed that $\beta = 0{\cdot}5$. The embedment depth $t = 120$ mm and the screw shank diameter $d = 12$ mm, therefore $\hat{t} = 10$. Predicted values of the slip modulus K based on these values are given in Table 2 for direct comparison with the experimental results. The experimental values are also plotted non-dimensionally in Figure 12 for varying angle of inclination θ with the model prediction shown as a continuous line. Although there is some scatter in the experimental results (9% difference between the two specimens on average) the model shows good agreement with the trend of the measured slip moduli. However, the agreement on magnitude is only reasonable as the model overestimates the measured slip moduli by an average of 20%. This overestimation can be explained to some extent by the imperfect assumption in the

Slip modulus K	α	0°	10°	20°	30°	40°	50°
Experimental loading							
Specimen 1	kN/mm per screw	23·0	27·0	27·3	29·7	32·3	40·0
Specimen 2	kN/mm per screw	22·5	27·5	27·2	27·3	41·4	49·0
Model prediction							
Predicted modulus	kN/mm per screw	32·2	32·3	33·6	37·1	42·8	48·3

Table 2. Push-off shear test results and predictions for 16×230 mm coach screws in GL28 timber

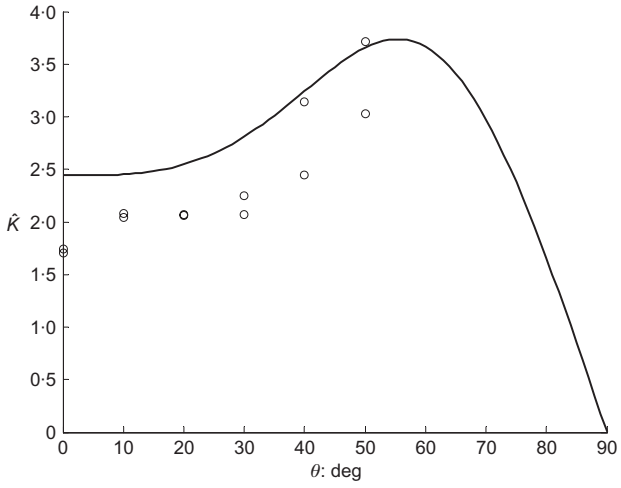

Figure 12. Comparison of predicted and measured slip modulus $\hat{K}$ for large-scale shear tests ($\hat{t} = 10$, $\hat{E} = 180$ and $\beta = 0{\cdot}5$)

model that the screw heads are fully rigidly held. It is worth noting that the significant thinning of the concrete slab between screws (from 100 mm to 50 mm) owing to the use of the troughed Holorib steel decking will add additional flexibility.

3.2. Small-scale tests: 6 × 50 mm coach screws in balsa wood

3.2.1. Experimental method. Single-sided shear tests were conducted in balsa specimens with three 6 × 50 mm coach screws inserted at an angle θ to the normal of the grain direction. Tests were conducted for the range $\theta = 0°$ to 60° (the practical limit for the chosen test configuration), in increments of 10°. A minimum of five tests were conducted at each angle. The test configuration is shown in Figure 13. For these small-scale tests a 6 mm thick steel plate was substituted for the in situ cast concrete slab used in the large-scale tests. This plate provided the equivalent moment fixity required for the head of the screws. The slip modulus of each specimen was estimated from the linear portion of the initial measured load/slip response. Further details of these small-scale tests are given by Stanislaus (2008).

3.2.2. Comparison of model with experimental results. The Young's modulus of the balsa wood specimens tested was not directly measured, but may be estimated using the scaling rules and results reported by Tagarielli *et al.* (2005). The modulus of wood parallel to the grain E_p is dominated by stretching of the cell walls and therefore scales in proportion to the density (in contrast, for loading transverse to the grain the cell walls tend to bend and the stiffness scales in proportion to the density cubed).

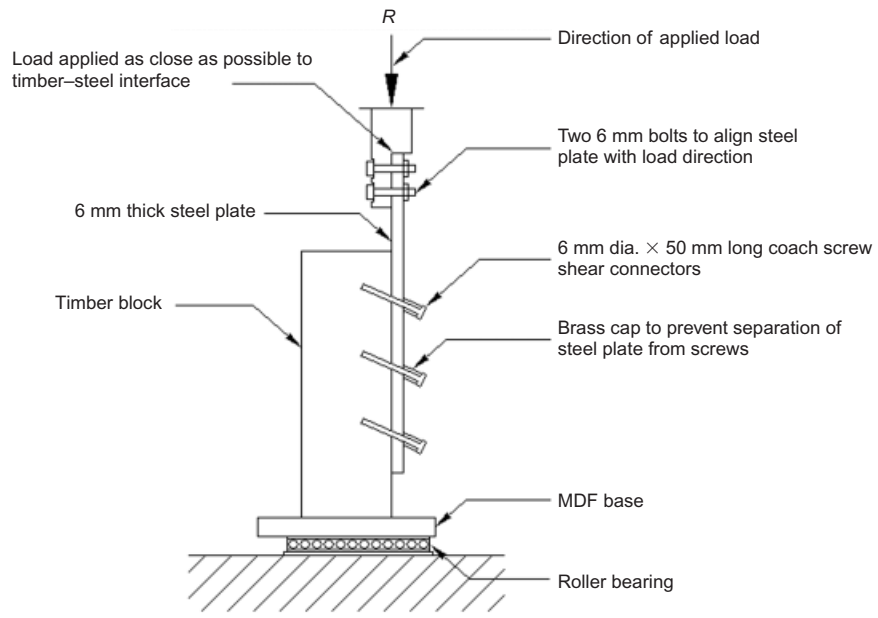

Figure 13. Test configuration for 6×50 mm coach screws in balsa wood

Tagarielli *et al.* (2005) reported a value of $E_p = 0{\cdot}845$ GPa at a reference density of 100 kg/m^3. The measured average density of the balsa used in the small-scale tests was 124 kg/m^3 and therefore $E_p \sim 1{\cdot}0$ GPa. Since the foundation modulus is expected to scale directly with E_p, $k_p \sim 85$ N/mm^2 is therefore estimated and hence $\hat{E} = 2350$. The embedment depth $t = 28$ mm and the screw shank diameter $d = 4$ mm, therefore $\hat{t} = 7$. It is again assumed that $\beta = 0{\cdot}5$ (but note that for these values $\hat{E}$ and $\hat{t}$ the model prediction is insensitive to the value of β). The experimental values of slip modulus are plotted non-dimensionally as $\hat{K}$ in Figure 14 (as circles, with filled squares to indicate mean values) for varying angle of inclination θ with the model prediction shown as a continuous line. In this case the combination of a very low foundation modulus and relatively short embedment length mean that the screws do not develop significant axial tension and increasing inclination actually reduces the slip modulus. There is significant scatter in the experimental results; this may be attributed to early inelastic crushing of the balsa, even at the very low loads used to determine the slip modulus. However, the model again shows reasonable agreement with the magnitude and trend of the measured slip moduli (the model again overestimates the experimental results by 20% on average).

4. CONCLUSION

A model is proposed for calculating the slip modulus of inclined screw shear connectors. Such connectors have application in timber–concrete composite construction; the slip modulus determines the degree of composite action that is achieved. The experimental observation that inclining screws in the direction of shear can give increased slip modulus is predicted by the model. The model assumes the screw behaves as a beam resting on two orthogonal spring foundations; it takes account of the length and inclination of the screw. Two sets of experiments carried out by the authors provide preliminary validation of the model. Good agreement is found with the trend and reasonable agreement with the magnitude of these experimental results. The model overestimates the magnitude by ~20%; this may be attributed to some extent to the imperfect assumption of a completely rigidly held screw head.

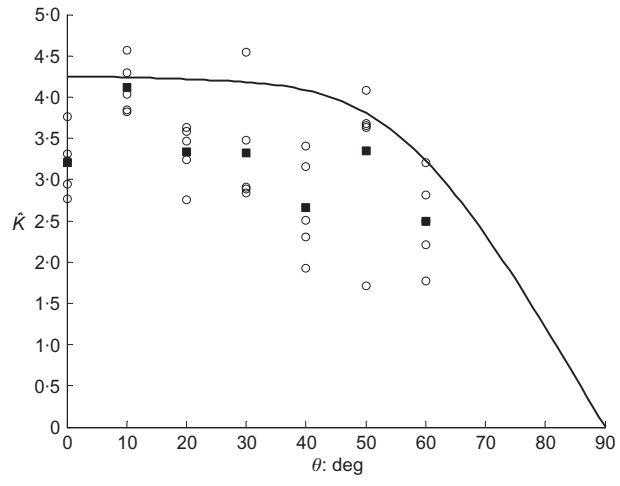

Figure 14. Comparison of predicted and measured slip modulus $\hat{K}$ for small-scale shear tests ($\hat{t} = 7$, $\hat{E} = 2350$ and $\beta = 0{\cdot}5$)

ACKNOWLEDGEMENTS

The work presented in this paper formed part of a research project at the University of Cambridge Department of Engineering. The generous contributions to the project of the Cambridge Commonwealth Trust, Ramboll, Lilleheden Ltd and Richard Lees Steel Decking Ltd are gratefully acknowledged.

REFERENCES

Bathon L and Clouston P (2004) Experimental and numerical results on semi-prestressed wood–concrete composite floor systems for long span applications. *Proceedings of the 8th World Conference on Timber Engineering*, Lahti, Finland, **1**, 339–344.

Blass HJ and Schmid M (2001) Self-tapping screws as reinforcement perpendicular to the grain in timber connections. *International RILEM Symposium on Joints in Timber Structures*, Stuttgart, Germany, 163–172.

BSI (British Standards Institution) (2004) *Eurocode 5: Design of Timber Structures. Part 1·1: General Rules and Rules for Buildings*. BSI, London, BS EN 1995-1-1.

Ceccotti A, Fragiacomo M and Gutkowski R (2002) On the design of timber–concrete composite beams according to the new versions of Eurocode 5. *35th Meeting of the Working Commission W18–Timber Structures, International Council for Research and Innovation in Building and Construction, Kyoto, Japan*, 10–24.

Clouston P, Civjan S and Bathon I (2004) Experimental behaviour of a continuous metal connector for a wood–concrete composite system. *Forest Products Journal* **54(6)**: 76–84.

Fontana M and Frangi A (2003) Elasto-plastic model for timber–concrete composite beams with ductile connection. *Structural Engineering International* **13(1)**: 47–57.

Gattesco N (1998) Strength and local deformability of wood beneath bolted connectors. *Journal of Structural Engineering* **124(2)**: 195–202.

Gattesco N and Toffolo I (2004) Experimental study on multiple-bolt steel-to-timber tension joints. *Materials and Structures* **37(2)**: 129–138.

Gelfi P, Giuriani E and Marini A (2002) Stud shear connection design for composite concrete slab and wood beams. *Journal of Structural Engineering* **128(12)**: 1544–550.

Hetenyi M (1946) *Beams on Elastic Foundation*, vol. XVI. University of Michigan Press, Michiagan.

Jensen LJ (2005) Quasi-non-linear fracture mechanics analysis of the double cantilever beam specimen. *Journal of Wood Science* **51(6)**: 566–571.

Jensen LJ and Gustafsson P-J (2004) Shear strength of beam splice joints with glued-in rods. *Journal of Wood Science* **50(2)**: 123–129.

Kuenzi EW (1951) *Theoretical Design of a Nailed or Bolted Joint Under Lateral Load*. USDA, Forest Service, Forest Products Laboratory, Research paper No. D1951.

Meierhofer U (1993) A timber/concrete composite system. *Structural Engineering International* **3(2)**: 104–107.

Patton-Mallory M, Pellicane PJ and Smith FW (1997) Modeling bolted connections in wood: review. *Journal of Structural Engineering* **123(8)**: 1054–1062.

Persaud R (2006) *The Structural Behaviour of a Composite Timber and Concrete Floor System Incorporating Steel Decking as Permanent Formwork*. PhD thesis, University of Cambridge Department of Engineering.

Persaud R and Symons D (2006) Design and testing of a timber and concrete floor system. *The Structural Engineer* **84(4)**: 22–30.

Santos CL, de Jesus AMP, Morais JJL and Lousada JLPC (2010) A comparison between the EN 383 and ASTM D5764 test methods for dowel-bearing strength assessment of wood: experimental and numerical investigations. *Strain* **46(2)**: 159–174.

Stanislaus H (2008) *Timber and concrete construction*. MEng project report, University of Cambridge, Department of Engineering.

Steinberg E, Selle R and Faust T (2003) Connectors for timber–lightweight Concrete Composite structures. *Journal of Structural Engineering* **129(11)**: 1538–1545.

Symons DD, Persaud R and Stanislaus H (2010) Strength of inclined screw shear connections for timber and concrete composite construction. *The Structural Engineer* **88(1)**: 25–32.

Tagarielli VL, Deshpande VS, Fleck NA and Chen C (2005) A constitutive model for transversely isotropic foams, and its application to the indentation of balsa wood. *International Journal of Mechanical Sciences* **47(4/5)**: 666–686.